Mathematical and Computer Modelling 58 (2013) 300–305

Contents lists available at SciVerse ScienceDirect

Mathematical and Computer Modelling

journal homepage: www.elsevier.com/locate/mcm

Computer simulation of electron energy state spin-splitting in nanoscale InAs/GaAs semiconductor quantum rings

Yiming Li

Parallel and Scientific Computing Laboratory, Department of Electrical and Computer Engineering, National Chiao Tung University, Hsinchu 300, Taiwan

ARTICLE INFO

Keywords:
Semiconductor nanostructure
InAs/GaAs
Quantum rings
Spin–orbit interaction
Energy spectra
Nonlinear Schrödinger equation
Nonlinear eigenvalue problem
Nonlinear iterative method
Monotone convergence

ABSTRACT

In this paper, we model and computationally investigate the effect of spin–orbit interaction on the electron energy spectra for nanoscale semiconductor quantum rings. Our three-dimensional mathematical model considers the effective one-electron band Hamiltonian, the energy- and position-dependent electron effective mass approximation, and the spin-dependent Ben Daniel–Duke boundary conditions. The nonlinear iterative method is applied to solve the corresponding nonlinear eigenvalue problem, which converges monotonically for all energy states. Physically, it is found that the spin-dependent boundary conditions lead to a spin-splitting of the electron energy states with non-zero angular momentum in nanoscale InAs/GaAs quantum rings. The spin-splitting is strongly dependent upon the dimension of the explored quantum ring and is dominated by the inner radius, the base radius, and the height of the quantum ring. Under zero magnetic fields, the spin-splitting energy is decreased when the radius is increased. Meanwhile, it is greater than that of the InAs/GaAs quantum dot and demonstrates an experimentally measurable quantity (up to 2 meV) for relatively small semiconductor quantum rings.

1. Introduction

Nanoscale semiconductor quantum structures have recently been of great interest [1–4]. Among these structures, quantum rings are known to possess interesting physical properties and have potential applications to the field of nanoelectronics and optics [5–10]. Electron spin plays an important role in the manipulation of energy states and modifies the intrinsic property of nanoscale quantum rings. In semiconductor spintronics, the spin-dependent electron confinement and the spin–orbit interaction impact the energy and electronic properties of semiconductor nanostructures [11–19]. Different theoretical models have been proposed to study the spin–orbit interaction for various quantum structures [11–23]. Three-dimensional (3D) modeling and computer simulation will accurately estimate effects of geometry and spin–orbit interactions on the energy state in nanoscale semiconductor quantum rings.

In this paper, we computationally explore the effect of spin–orbit interaction on the electron energy states in nanoscale semiconductor quantum rings. The effective one-band Hamiltonian approximation with the spin-dependent Ben Daniel–Duke boundary conditions is firstly formulated, where a hard-wall 3D confinement potential (i.e., a barrier with finite height) is considered. The hard-wall confinement is physically induced by a realistic discontinuity of the conduction bands at the edge of a semiconductor quantum ring. To efficiently solve the corresponding nonlinear Schrödinger equation, the nonlinear iterative method [24–26] is applied to calculate the energy states and then wavefunctions are solved numerically. Based upon the monotone property of the electron's effective mass with respect to each energy state, it can be shown that the numerical algorithm converges to each energy state monotonically. This solution methodology was developed in our recent work for the simulation of semiconductor quantum nanostructures [23–27]. A mathematical proof of the

E-mail address: ymli@faculty.nctu.edu.tw.

0895-7177/$ – see front matter © 2012 Elsevier Ltd. All rights reserved.
doi:10.1016/j.mcm.2012.11.005

convergence property of the nonlinear iterative method in semiconductor quantum dot simulation has also been reported recently [28]. It is robust and cost-effective in the numerical simulation of the spin-dependent semiconductor quantum ring. Due to a significant spin–orbit interaction in the nonsimply connected torus topology, an experimentally measurable spin-splitting is computationally observed in nanoscale InAs/GaAs quantum rings. The spin-splitting depends on the variations of geometrical dimension which are dominated by the inner radius, the base radius, and the height of the quantum ring. Under zero magnetic fields, it is found that the examined InAs/GaAs quantum ring can approximately produce 2 meV spin-splitting of the excited electronic states when the inner radius is small and the ratio of the height and the base radius is greater than 1. It is substantially greater than that of the InAs/GaAs quantum dot (about 1 meV) [10,15].

This article is organized as follows. Section 2 introduces the 3D mathematical model and the corresponding nonlinear Schrödinger equation for the semiconductor quantum ring. Section 3 describes the numerical simulation method. Section 4 reports the computed results illustrating the effect of spin–orbit interaction on the electron energy spectra for the small InAs/GaAs quantum rings. Section 4 draws conclusions.

2. Modeling energy state with spin-dependent boundary conditions

Considering electrons confined in a system of the 3D quantum ring and applying an effective one-electron band Hamiltonian, we have [10,15,23–27]

$$\hat{H} = \hat{H}_0 + \hat{V}_{so}(\mathbf{r}), \tag{1}$$

where $\hat{H}_0$ is the Hamiltonian of the system without the spin–orbit interaction and $V_{so}(\mathbf{r})$ indicates the spin–orbit interaction for the conduction band electrons. The expression for $\hat{H}_0$ is given by

$$\hat{H}_0 = -\frac{\hbar^2}{2}\nabla_{\mathbf{r}}\left(\frac{1}{m(E,\mathbf{r})}\right)\nabla_{\mathbf{r}} + V(\mathbf{r}), \tag{2}$$

where $\nabla_{\mathbf{r}}$ stands for the spatial gradient. $m(E,\mathbf{r})$ is the energy- and position-dependent electron effective mass

$$\frac{1}{m(E,\mathbf{r})} = \frac{P^2}{\hbar^2}\left[\frac{2}{E + E_g(\mathbf{r}) - V(\mathbf{r})} + \frac{1}{E + E_g(\mathbf{r}) + \Delta(\mathbf{r}) - V(\mathbf{r})}\right]. \tag{3}$$

In Eq. (3), $V(\mathbf{r})$ is the confinement potential, and $E_g(\mathbf{r})$ and $\Delta(\mathbf{r})$ stand for the position-dependent band gap and the spin–orbit splitting in the valence band, respectively. P in Eq. (3) is the momentum matrix element. The spin–orbit interaction for the conduction band electrons $V_{so}(\mathbf{r})$ is given by [13,15]

$$\hat{V}_{so}(\mathbf{r}) = i\nabla\beta(E,\mathbf{r})\cdot[\widehat{\sigma}\times\nabla], \tag{4}$$

where $\beta(E,\mathbf{r})$ is the spin–orbit coupling parameter and $\widehat{\sigma} = \{\sigma_{\mathbf{x}}, \sigma_{\mathbf{y}}, \sigma_{\mathbf{z}}\}$ is the vector of the Pauli matrices. The energy- and position-dependent $\beta(E,\mathbf{r})$ has the form

$$\beta(E,\mathbf{r}) = \frac{P^2}{2}\left[\frac{1}{E + E_g(\mathbf{r}) - V(\mathbf{r})} - \frac{1}{E + E_g(\mathbf{r}) + \Delta(\mathbf{r}) - V(\mathbf{r})}\right]. \tag{5}$$

For a system of quantum rings with sharp discontinuity on the conduction band interfaces between the quantum ring (material 1) and the semiconductor matrix (material 2), the hard-wall confinement potential is

$$V(\mathbf{r}) = \begin{cases} 0, & \mathbf{r} \in \texttt{material 1} \\ V_0, & \mathbf{r} \in \texttt{material 2}, \end{cases} \tag{6}$$

where V_0 is the structure band offset. Combining the Hamiltonian in Eqs. (1), (2) and (4), and taking an integration of this Schrödinger equation with respect to the direction which is perpendicular to interfaces of the system, the spin-dependent Ben Daniel–Duke boundary conditions for the electron wavefunction $\Psi(\mathbf{r})$ is written as follows:

$$\begin{aligned} &\Psi_{\texttt{material 1}}(\mathbf{r}_s) = \Psi_{\texttt{material 2}}(\mathbf{r}_s) \\ &\left\{\frac{\hbar^2}{2m(E,\mathbf{r}_s)}\nabla - i\beta(E,\mathbf{r}_s)[\widehat{\sigma}\times\nabla]\right\}_n \Psi(\mathbf{r}_s) = C_0, \end{aligned} \tag{7}$$

where C_0 is some constant, and $\mathbf{r}_s$ denotes the position of interfaces of the system. The spin-dependent boundary condition is formed from the difference between the spin–orbit interaction parameters in the quantum ring and the semiconductor environment matrix. We note that the expressions of electron effective mass in Eq. (3), the spin–orbit coupling parameter in Eq. (5), and the equations of the Ben Daniel–Duke boundary condition in Eq. (7) are all energy- and position-dependent relationships in this study.

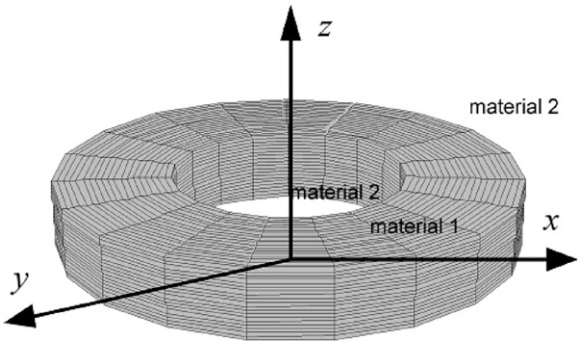

Fig. 1. A three-dimensional plot of the disk-shaped semiconductor quantum ring.

The quantum ring, shown in Fig. 1, is with the inner radius R_{in}, the radius R_0, and the thickness z_0 in the cylindrical coordinate (R, ϕ, z). The origin of the quantum system is at the center of the quantum ring and the z axis is chosen along the rotation axis. Since the quantum system is cylindrically symmetric, the wavefunction is expressed as

$$\Psi(\mathbf{r}) = \Phi(R, z)\exp(il\phi), \tag{8}$$

where $l = 0, \pm 1, \pm 2, \ldots$ is the electron orbital quantum number and the original model problem is now in the (R, z) coordinates. From Eqs. (1)–(6) and (8), we obtain the equations

$$-\frac{\hbar^2}{2m_1(E)}\left(\frac{\partial^2}{\partial R^2}+\frac{\partial}{R\partial R}+\frac{\partial^2}{\partial z^2}-\frac{l^2}{R^2}\right)\Phi_1(R,z) = E\Phi_1(R,z), \quad \forall (R,z) \in \text{material 1} \tag{9}$$

and

$$-\frac{\hbar^2}{2m_2(E)}\left(\frac{\partial^2}{\partial R^2}+\frac{\partial}{R\partial R}+\frac{\partial^2}{\partial z^2}-\frac{l^2}{R^2}\right)\Phi_2(R,z) + V_0\Phi_2(R,z) = E\Phi_2(R,z), \quad \forall (R,z) \in \text{material 2}. \tag{10}$$

The problem is symmetry along the z axis, so the spin-dependent boundary conditions in Eq. (7) are given by $\Phi_1(R, z) = \Phi_2(R, z)$, $z = f(R)$, and

$$\begin{aligned}&\frac{1}{m_1(E)}\left\{\frac{\partial\Phi_1(R,z)}{\partial R}+\frac{df(R)}{dR}\frac{\partial\Phi_1(R,z)}{\partial R}\right\}_{z=f(R)}\\ &-\frac{1}{m_2(E)}\left\{\frac{\partial\Phi_2(R,z)}{\partial R}+\frac{df(R)}{dR}\frac{\partial\Phi_2(R,z)}{\partial R}\right\}_{z=f(R)}+\frac{2\sigma(\beta_1-\beta_2)}{\hbar^2}\frac{l}{R_0}\Phi_1(R_0,z)=0,\end{aligned} \tag{11}$$

where $z = f(R)$ is a generating contour of the quantum ring on the $\{R, z\}$ plane and σ refers to the electron spin polarization along the z direction.

3. Numerical calculation using the nonlinear iterative method

Dependence of the electron effective mass and spin–orbit coupling parameter on each energy state results in a nonlinear Schrödinger equation. The nonlinear Schrödinger equation complicates the process of analytical solution in the explored quantum ring. Therefore, the numerical approach to the solution of the nonlinear Schrödinger equation is advanced in the calculation of the electronic structure of InAs/GaAs quantum rings. The nonlinear iterative method [24–26] is applied to solve the problem above for the nanoscale InAs/GaAs quantum rings. Energy states and spin-splitting are numerically calculated without any fitting parameters. Starting from a given initial energy, the nonlinear iterative method globally calculates all bounded energies for the corresponding nonlinear algebraic eigenvalue problem. A computational procedure of the nonlinear iterative method is shown below:

Step 1. Set an initial energy E_0;
Step 2. Compute electron effective mass m with Eq. (3);
Step 3. Compute spin–orbit coupling parameter β with Eq. (5);
Step 4. Solve the approximated Schrödinger equation as well as the boundary conditions (9)–(11);
Step 5. Update the newer computed energy; and
Step 6. Calculate the error and back to *Step* 2.

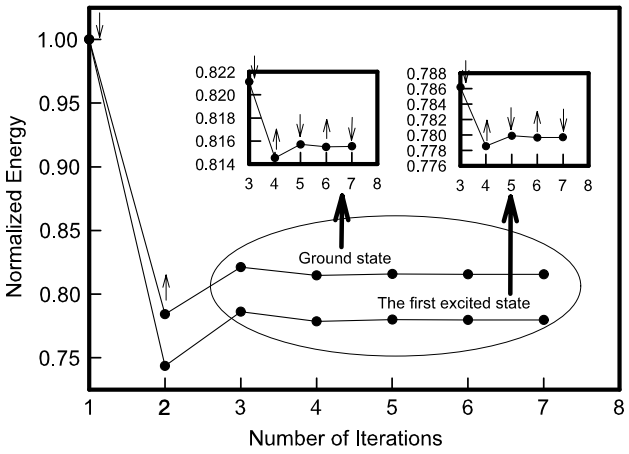

Fig. 2. The normalized energy sequence versus the number of iterations. Starting from a lower bound of energy (say, $E_0 = 0$ eV), the computed solutions can be cataloged into two different energy sequences. Both the increasing (upward arrows) and decreasing (downward arrows) energy sequences converge monotonically.

It could be shown that the energy sequence, shown in Fig. 2, converges monotonically based on a monotone operator theory. The insets of Fig. 2 exhibit the increasing and decreasing energy sequences for the ground (the left inset) and the first excited (the right one) energy states. To obtain the complete numerical solution of the Schrödinger equation in *Step* 4, the finite element (similarly we can discretize it with finite difference and finite volume methods) approximated Schrödinger equation with its boundary conditions leads to a generalized nonlinear algebraic eigenvalue problem [25]. With the proposed nonlinear iterative method above, the eigenvalues of the matrix eigenvalue problem are computed with the hybrid method [25], which integrates the multishift QR algorithm and the implicitly restarted Arnoldi method [25,29,30]. The iteration will be terminated when the error of the computed energy is convergent to a specified tolerance error. This method converges monotonically and is cost effective in the simulation of 3D quantum rings.

The energy spectrum of the quantum ring is a set of discrete energy states that is formed and numerated by a set of numbers (n, l, σ), where n is the nth solution of the problem with a fixed l and σ. For the same value of n, the parallel (antiparallel) orbital momentum, and spin, the energy states still have two-fold degeneracy (the well-known Kramers degeneracy). But nth states with antiparallel orbital momentum and spin are separated from the nth state with parallel orbital momentum and spin. For cylindrical quantum rings, a conventional notation nL_σ for the electron energy states is adopted, where $L = S, P, D, \ldots$ denotes the absolute value of l, and $\sigma = \pm 1$ refers to the electron spin directions corresponding to the electron angular momentum direction. For all calculations we choose the lowest energy states ($n = 1$).

4. Results and discussion

In the calculation of the electron energy spectra for InAs/GaAs quantum rings we choose the semiconductor band structure parameters for InAs as follows [10,15,23–25,27,26]. The energy gap is $E_{1g} = 0.42$ eV and the spin–orbit splitting $\Delta_1 = 0.48$ eV. The value of the nonparabolicity parameter $E_{1p} = 3m_0P_1^2/\hbar^2 = 22.2$ eV, where m_0 is the free electron effective mass. For GaAs, $E_{2g} = 1.52$ eV, $\Delta_2 = 0.34$ eV, and $E_{2p} = 24.2$ eV. The band offset is taken as $V_0 = 0.77$ eV. The spin-splitting effect is obviously zero for the lowest energy state $1S_{\pm 1}$. The dependence of the $1P$ energy level splitting

$$\Delta E_{1P} = E_{1P_{+1}} - E_{1P_{-1}}$$

on the ring size is shown in Fig. 3. Our calculation demonstrates a significant spin-splitting for ultrasmall semiconductor quantum rings. The splitting is strongly dependent on the ring radius and is decreased when the radius is increased. At the same time for the quantum ring with relatively small thickness the spin-splitting is small. This is a direct result of the tunneling of the electron wavefunction into the barrier along the z-direction. It is also related to the energy dependence of the electron effective mass and the spin–orbit coupling parameters. To clarify the result we have compared the "weight" of the electron wavefunction inside and outside the quantum ring [15,23,27]. For the quantum ring with small thickness the electron "spreads" out of the quantum ring, and the energy level properties are controlled by the band parameters of the GaAs matrix. Under this situation an effective difference of spin–orbit coupling parameters is smaller than $\beta_1(E = 0) - \beta_2(E = 0)$. When z_0 is increased the difference is also increased and then becomes z-independent. It results in the splitting effect being significant when z_0 is increased.

As shown in Fig. 3, the energy splitting for the state $1P$ depending on the ring size is defined as ΔE_{1P}, where the ring's inner radius is 10 nm [6–10]. Our approach demonstrates a significant spin-splitting (2 meV) for an ultrasmall quantum ring. It is larger than that of a quantum dot (1 meV) which was reported in our recent work [15,23]. For the small InAs/GaAs quantum ring ($z_0 = 2$ nm and $R = 6$ nm), the spin-splitting of the state $|l| = 1$ with different inner radii R_{in} is summarized in Table 1. It reports the variation of ΔE_{1P}, versus R_{in}. ΔE_{1P} is increased when the inner radius is decreased.

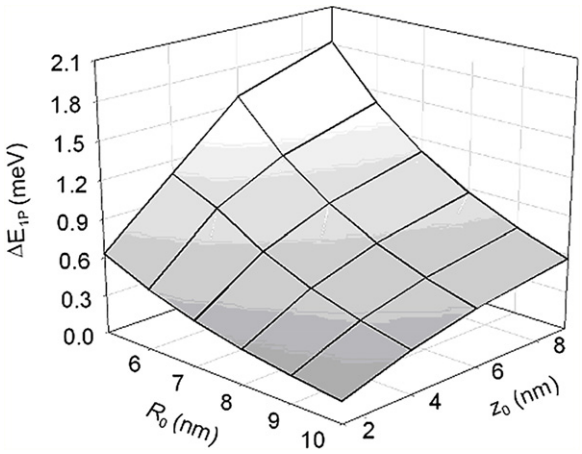

Fig. 3. The spin-splitting of $|l| = 1$ states for InAs/GaAs quantum rings with different base radii and heights, where the inner radius is chosen as 2 nm.

Table 1
The 1*P* energy level splitting versus R_{in}.

R_{in} (nm)	2	4	6	8	10
ΔE_{1P} (meV)	0.81	0.72	0.66	0.58	0.47

5. Conclusions

We have numerically studied the effect of spin–orbit interaction on the electron energy states for ultrasmall semiconductor quantum rings. It is found that the spin–orbit interaction can significantly modify the electron energy spectrum of InAs/GaAs semiconductor quantum rings. Under zero magnetic fields, an ultrasmall InAs/GaAs quantum ring approximately produces 2 meV spin-splitting of the excited electronic states which is substantially greater than that of a quantum dot (1 meV). The modeling and simulation presented here plays a starting point for estimation of the spin–orbit interaction effects in 3D semiconductor quantum rings. The spin–orbit interaction provides rich physics and is promising in nanoelectronic applications. We note that the effect of band offset V_0 on the energy state could be explored in the near future. Multiband and self-consistent potentials will also provide more accurate corrections.

Acknowledgment

This work was supported in part by the Taiwan National Science Council (NSC) under Contract No. NSC-100-2221-E-009-018.

References

[1] E. Zipper, M. Kurpas, J. Sadowski, M. Maska, Spin relaxation in semiconductor quantum rings and dots—a comparative study, Journal of Physics: Condensed Matter 23 (2011) 115302.
[2] J. Akinaga, H. Ohno, Semiconductor spintronics, IEEE Transactions on Nanotechnology 1 (2002) 19–31.
[3] M. Bayer, P. Hawrylak, K. Hinzer, S. Fafard, M. Korkusinski, Z.R. Wasilewski, O. Stern, A. Forchel, Coupling and entangling of quantum states in quantum dot molecules, Science 291 (2001) 451–453.
[4] A.D. Yoffe, Semiconductor quantum dots and related systems: electronic, optical, luminescence and related properties of low dimensional systems, Advances in Physics 50 (2001) 1–208.
[5] M. Abbarchi, A. Mastrandrea, A. Vinattieri, S. Sanguinetti, T. Mano, T. Kuroda, N. Koguchi, K. Sakoda, M. Gurioli, Photon antibunching in double quantum ring structures, Physical Review B 79 (2009) 085308.
[6] U.F. Keyser, C. Fuhner, S. Borck, R.J. Haug, Kondo effect in a few-electron quantum ring, Physical Review Letters 90 (2003) 196601.
[7] A. Fuhrer, S. Luscher, T. Ihn, T. Heinzel, K. Ensslin, W. Wegscheider, M. Bichler, Energy spectra of quantum rings, Nature 413 (2001) 822–824.
[8] A. Lorke, R. Johannes Luyken, A.O. Govorov, J.P. Kotthaus, J.M. Garcia, P.M. Petroff, Spectroscopy of nanoscopic semiconductor rings, Physical Review Letters 84 (2000) 2223.
[9] J.M. Garcia, G. Medeiros-Ribeiro, K. Schmidt, T. Ngo, J.L. Feng, A. Lorke, J. Kotthaus, P.M. Petroff, Intermixing and shape changes during the formation of InAs self-assembled quantum dots, Applied Physics Letters 71 (1997) 2014–2016.
[10] Y. Li, Numerical calculation of electron energy states for nanoscopic InAs/GaAs quantum rings, International Journal of Modern Physics C 14 (2003) 995–1006.
[11] G. Dresselhaus, Spin–orbit coupling effects in zinc blende structures, Physical Review 100 (1955) 580–586.
[12] A. Emperador, F. Pederiva, E. Lipparini, Spin- and localization-induced fractional Aharonov–Bohm effect, Physical Review B 68 (2003) 115312.
[13] S. Tarucha, T. Honda, D.G. Austing, Y. Tokura, K. Muraki, T.H. Oosterkamp, J.W. Janssen, Electronic states in quantum dot atoms and molecules, Physica E 3 (1998) 112–120.
[14] Y.A. Bychkov, E.I. Rashba, Oscillatory effects and the magnetic susceptibility of carriers in inversion layers, Journal of Physics C: Solid State Physics 17 (1984) 6039–6046.

[15] Y. Li, Voskoboynikov, C.P. Lee, S.M. Sze, O. Tretyak, Electron energy state spin-splitting in 3D cylindrical semiconductor quantum dots, The European Physical Journal B 28 (2002) 475–481.
[16] E.A. de Andrada e Silva, G.C. La Rocca, F. Bassani, Spin–orbit splitting of electronic states in semiconductor asymmetric quantum wells, Physical Review B 55 (1997) 16293–16299.
[17] A.G. Mal'shukov, K.A. Chao, Waveguide diffusion modes and slowdown of D'yakonov-Perel' spin relaxation in narrow two-dimensional semiconductor channels, Physical Review B 61 (2000) 2413–2416.
[18] P.N. Racec, Toma Stoica, Corneliu Popescu, Mihail Lepsa, Th. G. van de Roer, Physics of optimal resonant tunneling, Physical Review B 56 (1997) 3595–3597.
[19] A. Emperador, M. Pi, M. Barranco, A. Lorke, Far-infrared spectroscopy of nanoscopic InAs rings, Physical Review B 62 (2000) 4573–4577.
[20] D. Frustaglia, K. Richter, Spin interference effects in ring conductors subject to Rashba coupling, Physical Review B 69 (2004) 235310.
[21] F.E. Meijer, A.F. Morpurgo, T.M. Klapwijk, One-dimensional ring in the presence of Rashba spin–orbit interaction: derivation of the correct Hamiltonian, Physical Review B 66 (2002) 033107.
[22] A.G. Aronov, Y.B. Lyanda-Geller, Spin–orbit Berry phase in conducting rings, Physical Review Letters 70 (1993) 343–346.
[23] Y. Li, O. Voskoboynikov, C.P. Lee, S.M. Sze, O. Tretyak, A computational method for energy level spin splitting simulation in inas/gaas semiconductor quantum dots, International Journal of Modern Physics C 13 (2002) 453–464.
[24] Y. Li, O. Voskoboynikov, C.P. Lee, S.M. Sze, Computer simulation of electron energy levels for different shape InAs/GaAs semiconductor quantum dots, Computer Physics Communications 141 (2001) 66–72.
[25] Y. Li, Numerical calculation of electronic structure for three-dimensional nanoscale semiconductor quantum dots and rings, Journal of Computational Electronics 2 (2003) 49–57.
[26] Y. Li, An iterative method for single and vertically stacked semiconductor quantum dots simulation, Mathematical and Computer Modelling 42 (2005) 711–718.
[27] Y. Li, H.-M. Lu, Electron transition energy for vertically coupled InAs/GaAs semiconductor quantum dots and rings, Japanese Journal of Applied Physics 43 (2004) 2104–2109.
[28] H. Voss, Numerical calculation of the electronic structure for three-dimensional quantum dots, Computer Physics Communications 174 (2006) 441–446.
[29] K. Braman, R. Byers, R. Mathias, The multishift QR algorithm. Part II: aggressive early deflation, SIAM Journal on Matrix Analysis and Applications 23 (2002) 948–973.
[30] K. Braman, R. Byers, R. Mathias, The multishift QR algorithm. Part I: maintaining well-focused shifts and level 3 performance, SIAM Journal on Matrix Analysis and Applications 23 (2002) 929–947.